

Critical fluctuations in MnSi near T_c : A polarized neutron scattering study

S. V. Grigoriev,^{1,*} S. V. Maleyev,^{1,†} A. I. Okorokov,¹ Yu. O. Chetverikov,¹ R. Georgii,^{2,‡} P. Böni,² D. Lamago,² H. Eckerlebe,³ and K. Pranzas³

¹Petersburg Nuclear Physics Institute, Gatchina, St. Petersburg 188300, Russia

²ZWE FRM-II/E21, Technische Universität München, 85747 Garching, Germany

³GKSS Forschungszentrum, 21502 Geesthacht, Germany

(Received 16 August 2005; published 21 October 2005)

Results of polarized neutron small angle scattering in MnSi, a cubic itinerant magnet, near $T_c=28.8$ K are presented and analyzed. The diffuse scattering intensity looks like half-moons oriented along the incident neutron polarization. The sum of the intensities for two opposite polarizations form an anisotropic ring with weak spots, which below T_c transform into the Bragg peaks originating from the helical structure. These results are in semiquantitative agreement with the mean-field calculations based on the Bak-Jensen model that takes into account the hierarchy of the interactions: the exchange interaction, the isotropic Dzyaloshinskii-Moriya (DM) interaction and the weak anisotropic exchange (AE) interaction. The DM interaction is responsible for the scattering intensity concentrated in the half-moons. The AE interaction provides the anisotropy so that the correlation length diverges along $[111]$ only. The corresponding critical exponent is $\nu=0.62(1)$. The exponent of the Bragg intensity due to the helical structure at $T < T_c$ is $2\beta=0.44(1)$ where β is the exponent of the helix magnetization.

DOI: [10.1103/PhysRevB.72.134420](https://doi.org/10.1103/PhysRevB.72.134420)

PACS number(s): 75.40.-s, 61.12.Ex

I. INTRODUCTION

Incommensurate ordering and chirality in strongly correlated magnetic materials have recently gained much attention. In this regard noncentrosymmetric cubic MnSi is playing a particular role because it is one of the very few systems with very peculiar properties. Its magnetic structure is the left-handed spiral oriented along $\langle 111 \rangle$ axes with a period $d \approx 18$ nm resulting from the Dzyaloshinskii-Moriya interaction (DMI) due to noncentrosymmetric crystal structure $P2_13$.^{1,2} This single-handed degree of freedom facilitates the interpretation of experiments significantly. In addition attention is focused on MnSi because it is a model system for itinerant ferromagnetism characterized by paramagnetic moments that are much larger than the ordered moment below the transition.³ Therefore one may conclude that MnSi is close to the quantum critical point.⁴ Last but not least, the recent discovery of non-Fermi-liquid⁵ and a possible liquid-crystal-like state⁶ above a pressure $p_c \approx 14.6$ kbar have sparked a significant interest in the magnetic properties of MnSi.

As a result of the chiral symmetry of the order parameter a universality class of the second order transition with critical exponents was proposed⁷ and confirmed recently by polarized neutron scattering in triangular lattice antiferromagnet CsMnBr₃.^{8,9} Inelastic neutron scattering experiments near T_c (Ref. 10) have shown that critical dynamics in MnSi is strongly affected by the chirality of the magnetic fluctuations leading to a critical exponent ν that is rather close to the expected chiral symmetry.⁷

In this paper we present results of the small-angle polarized neutron scattering study of critical fluctuations in MnSi at ambient pressure. We demonstrate that the magnetic critical scattering is arranged on the spheres around the nuclear Bragg peaks. However very close to T_c the cubic anisotropy

plays a significant role. As a result the correlation length diverges along $\langle 111 \rangle$ directions only. This situation resembles closely the similar observation near the critical pressure but in the last case the correlation length was not measured.⁶ We give the explanation of these phenomena based on the Bak-Jensen model,¹¹ which takes into account the conventional exchange interaction, the DM interaction and the anisotropic exchange (AE) interaction. This model is qualitatively correct both near T_c and at critical pressure p_c as it catches the main symmetry features of the problem.

II. MEASUREMENTS

The used sample was a disk with 20 mm diameter and 2 mm thickness cut from a single crystal of MnSi grown at Ames Laboratory. Its structural mosaic of 0.22° was determined with the neutron spectrometer “Reflex” at FZ Jülich (Germany). The small-angle polarized neutron scattering (SAPNS) experiments were performed at the SANS-2 facility of the FRG-1 research reactor in Geesthacht (Germany). The beam of polarized neutrons ($P_i=0.95$) was used with a wavelength $\lambda=0.58$ nm, which is above d spacing of MnSi, so only magnetic scattering can be observed. The wavelength spread and the beam divergence were $\Delta\lambda/\lambda=0.1$ and 2.5 mrad, respectively. The scattered neutrons were detected with a position sensitive detector with 128×128 pixels and a spatial resolution of 4.4 mm. A q -range from 6×10^{-2} to 1 nm^{-1} was explored. The incident beam was directed along $[1\bar{1}0]$, so that the vectors parallel to $[111]$ and $[11\bar{1}]$ were in the scattering plane and perpendicular to the beam. The guide magnetic field of 1 mT was in this plane along $[11\bar{2}]$, i.e., perpendicular to $[111]$. The temperature was measured with accuracy better than 0.05 K.

Maps of the SAPNS intensities below and above $T_c=28.82(2)$ for two neutron polarizations along (“up”) and

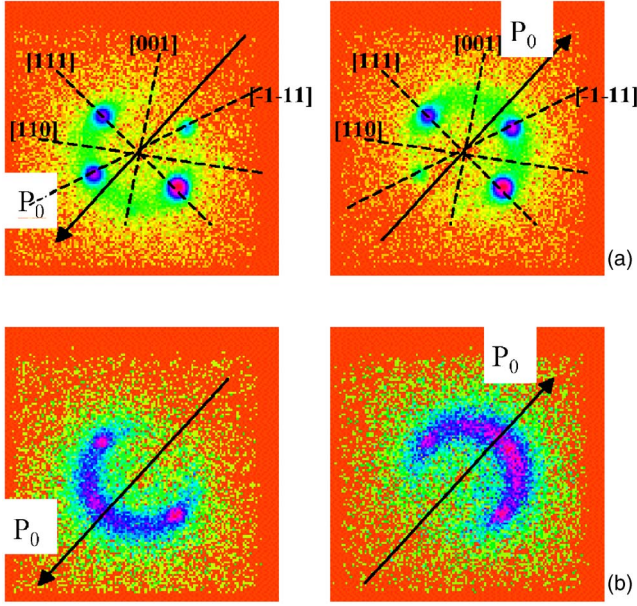


FIG. 1. (Color online) Maps of the SAPNS intensities for the polarization \mathbf{P}_i parallel to the $[11\bar{2}]$ direction, along the guide field (left) and opposite to it (right), $T = T_c - 0.1$ K (a), $T = T_c + 0.2$ K (b).

opposite (“down”) the guide field are shown in Fig. 1. Below T_c four Bragg peaks with $k = 0.39 \text{ nm}^{-1}$ and with different intensities are visible. They are the reflections from the domains oriented along $[111]$ and $[1\bar{1}\bar{1}]$. This is possible due to the large magnetic mosaic, as in the ideal case the Bragg condition would be only fulfilled for one reflection. In our geometry it is the $(11\bar{1})$ peak. The peaks at $\mathbf{k} = (111)$ and $\mathbf{k} = (\bar{1}\bar{1}\bar{1})$ are polarization independent, as \mathbf{k} is perpendicular to $\mathbf{P}_i \parallel [11\bar{2}]$. Reflections with $\mathbf{k} = (11\bar{1})$ and $\mathbf{k} = (\bar{1}\bar{1}\bar{1})$ depend on \mathbf{P}_i as expected for helices with the Dzyaloshinskii vector along \mathbf{q} . The intensity between the peaks (half-moons) is induced by the critical fluctuations. Above T_c , there are such half-moons only. In sum they compose a ring with the maximal intensity at $q = k$. There are weak spots on these half-moons corresponding to the former Bragg peaks. The intensity along the ring at $q = k$ and $T = T_c + 0.3$ K is shown in Fig. 2. The maxima of the measured intensity corresponds to the weak spots observed on the ring along the $\langle 111 \rangle$ in Fig. 1(b). As will be shown below the longitudinal q -scan of the scattering intensity at $T > T_c$ is well described by the Lorentzian. No contamination of the Bragg peaks, described by the Gaussian, is observed at $T > T_c$. Thus, we found that the critical scattering is maximal along $\langle 111 \rangle$ axes and is restricted along other directions which shows the importance of the anisotropic exchange interaction above T_c . To describe these experimental findings the following theory was developed.

III. MEAN-FIELD THEORY

A theoretical description of the paramagnetic fluctuations in cubic system with the Dzyaloshinskii-Moriya interaction

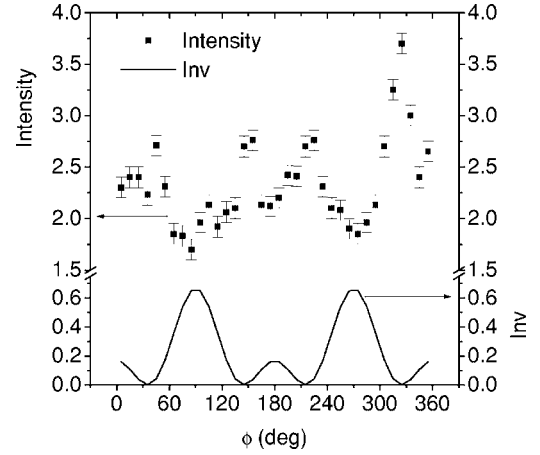


FIG. 2. Dependence of the scattering intensity (dots) and the cubic invariant (solid line) on the angle ϕ seen from the $[110]$ direction. The strong maximum of the intensity at $\phi \approx 325^\circ$ corresponds to the most intensive Bragg peak below T_c in the $[11\bar{1}]$ direction.

(DMI) starts, according to Ref. 11, with the bilinear part of the free energy density of the form

$$W(\mathbf{q}) = \left(\frac{B}{2}(q^2 + \kappa_0^2) \delta_{\alpha\beta} + iD \epsilon_{\alpha\beta\gamma} q_\gamma \right) S_{\mathbf{q}}^\alpha S_{-\mathbf{q}}^\beta + \frac{F}{2} (q_x^2 |S_{\mathbf{q}}^x|^2 + q_y^2 |S_{\mathbf{q}}^y|^2 + q_z^2 |S_{\mathbf{q}}^z|^2), \quad (1)$$

where the first, second, and third term correspond to the isotropic exchange, the DM interaction, and the AE interaction, respectively. $\kappa_0^2 = C(T - T_{c0})$ and T_{c0} are nonrenormalized square of the inverse correlation length and the transition temperature, respectively. As is well known the DM interaction and AE interaction are of first and second order in the spin-orbit interaction. Thus, we have $B > Da > F$, where a is the lattice constant. In the exchange approximation for the magnetic susceptibility we have the well-known expression $\chi_{\alpha\beta}^{(0)} = \chi_0 \delta_{\alpha\beta}$, and $\chi_0 = T/[B(q^2 + \kappa_0^2)]$ and using Eq. (1) for the susceptibility tensor we get

$$\chi_{\alpha\beta}(\mathbf{q}) = \chi_0(\mathbf{q}) \delta_{\alpha\beta} + \chi_0(\mathbf{q}) K_{\alpha\mu}(\mathbf{q}) \chi_{\mu\beta}(\mathbf{q}), \quad (2)$$

where the tensor $K = K^A + K^S$. Its antisymmetric part $K_{\mu\beta}^A = -i(D/T) q_\gamma \epsilon_{\gamma\mu\beta}$. For the symmetric part we have $K_{xx}^S = -(F/B) q_x^2$, etc.

The solution of Eq. (2) has the form

$$\chi_{\alpha\beta} = \frac{\chi_0}{\text{Det}} \left[\delta_{\alpha\beta} - \frac{2ikqD|D|}{q^2 + \kappa_0^2} \hat{q}_\gamma \epsilon_{\gamma\alpha\beta} - \left(\frac{2kq}{q^2 + \kappa_0^2} \right)^2 \hat{q}_\alpha \hat{q}_\beta \right], \quad (3)$$

where $\hat{q} = \mathbf{q}/q$, $k = |D|/B = 2\pi/d$ and d is the length of the spiral. Here, in the numerator we omitted small terms of the order $Fq_{x,y,z}^2/[B(q^2 + \kappa_0^2)]$ and

$$\text{Det} = 1 - \left(\frac{2kq}{q^2 + \kappa_0^2} \right)^2 - \frac{4k^2q^4}{(q^2 + \kappa_0^2)^3} \frac{F}{B} (\hat{q}_x^4 + \hat{q}_y^4 + \hat{q}_z^4), \quad (4)$$

here we retain only one term proportional to the small ratio F/B as it has cubic symmetry that breaks the full rotational symmetry of the problem. It is responsible for the orientation of the critical fluctuations with respect to the cubic axes. Using these equations we can write

$$\begin{aligned} \chi_{\alpha\beta} &= \frac{T}{BZ} \left((q^2 + \kappa_1^2 + k^2) \delta_{\alpha\beta} - 2i \frac{D}{|D|} kq_\gamma \epsilon_{\gamma\alpha\beta} \right. \\ &\quad \left. - \frac{(2qk)^2}{q^2 + \kappa_1^2 + k^2} \hat{q}_\alpha \hat{q}_\beta \right), \\ Z &= [(q+k)^2 + \kappa_1^2] \left((q-k)^2 + \kappa_1^2 \right. \\ &\quad \left. - \frac{q^2k^2}{q^2 + \kappa_1^2 + k^2} \frac{F}{B} (\hat{q}_x^4 + \hat{q}_y^4 + \hat{q}_z^4) \right), \end{aligned} \quad (5)$$

where $\kappa_1^2 = \kappa_0^2 - k^2 = C(T - T_{c1})$ and $T_{c1} = T_{c0} - k^2/C$. As the ra-

tio $|F|/B$ is very small the last term in the expression for Z is important very close to T_c only. As a result for $\kappa_1^2 > |F|/B$ critical fluctuations are maximal at the sphere $q=k$ and uniformly distributed at its surface. However very close to T_c , when $\kappa_1^2 \leq |F|/B$ the last term determines the form of the critical fluctuations.

The expression $\{\hat{q}^4\} = \hat{q}_x^4 + \hat{q}_y^4 + \hat{q}_z^4$ is a cubic invariant. It has two extrema equal to 1 and 1/3 for \mathbf{q} along the edges and the diagonals of the cubic unit cell, respectively. As a result for $F > 0$ we have a transition to a state with the helix axes along the edges [FeGe (Ref. 16)] and for $F < 0$ along the diagonals [MnSi (Ref. 1)]. In the last case we get

$$Z = [(q+k)^2 + \kappa^2] \left[(q-k)^2 + \kappa^2 + \frac{k^2|F|}{2B} \left(\{\hat{q}^4\} - \frac{1}{3} \right) \right], \quad (6)$$

where $\kappa^2 = \kappa_1^2 + k^2|F|/(6B)$. Here, in the first factor and in the last term we neglected a small difference between κ_1^2 and κ^2 and set $q=k$, respectively. In this approximation for the scattering of polarized neutrons using standard methods (see, for example, Ref. 12) we obtain

$$\frac{d\sigma}{d\Omega} = \frac{[rf(\mathbf{q})]^2 T}{[B(q+k)^2 + \kappa^2]} \frac{k^2 + q^2 + \kappa^2 - 2k\mathbf{q}\mathbf{P}_i}{(q-k)^2 + \kappa^2 + [F|k^2/(2B)](\{\hat{q}^4\} - 1/3)}, \quad (7)$$

where $r = 5.410 \times 10^{-13}$ cm, $f(\mathbf{q})$ is the magnetic form factor of the unit cell, \mathbf{P}_i is the neutron polarization, and we have taken into account that D is negative, as the helix is the left-handed one.¹

Equations (5)–(7) were derived in the mean-field approximation but they catch the main features following from the symmetry of the problem: (i) The dependence of the cross section on the polarization is a result of the DMI in complete agreement with the general theory.¹² In the case of MnSi the Dzyaloshinskii vector is directed along \mathbf{q} and the chiral part of the cross section is proportional to $\cos \phi$ where ϕ is the angle between \mathbf{P}_i and \mathbf{q} so the scattering almost vanish if $\phi = 0^\circ$. (ii) Not very close to T_c the maximum of the scattering intensity lies on the sphere $q=k$. Both (i) and (ii) are in full agreement with the results shown in Fig. 1. (iii) Due to the AE interaction the scattering near T_c is anisotropic and is maximal along diagonals, which are easy directions. It should be noted that qualitatively the last two features were mentioned by Brazovskii,¹³ who predicted the first order transition if one neglects the AE interaction. It is convenient to determine the so-called polarization of the scattering as¹⁴

$$P_s = \frac{\sigma(\mathbf{P}_i) - \sigma(-\mathbf{P}_i)}{\sigma(\mathbf{P}_i) + \sigma(-\mathbf{P}_i)} = - \frac{2kqP_i \cos \phi}{q^2 + k^2 + \kappa^2}. \quad (8)$$

IV. RESULTS AND DISCUSSION

For comparison with the above developed theory we added in Fig. 2 the cubic invariant $\text{Inv} = \{\hat{q}^4\} - 1/3$. The correlation between the positions of the maxima of the measured intensity (dots) and the minima of the calculated Inv (solid lines) are clearly observed demonstrating the importance of the anisotropic exchange interaction near T_c . Simultaneously we observed that within the error bars $P_s \sim \cos \phi$ in agreement with Eq. (8).

Figure 3 shows the temperature dependence of the (111) Bragg peak and the maximal intensity of the critical fluctuations along the easy [111] and hard [001] directions. In the last case critical fluctuations below T_c are clearly seen. The temperature dependence of the polarization P_s as determined by Eq. (8) is shown too. The q scans along the easy direction across the ring for the intensity (squares) and the polarization (circles) P_s are shown in Fig. 4. It is seen that Eqs. (7) and (8) (solid lines) describe the data well.

We present a theoretical description of the critical fluctuations in the mean-field approximation that correctly tackles the symmetry of the problem but cannot describe the temperature dependence of the relevant quantities. If one neglects the AE interaction the theory predicts a first order transition.¹³ However, apparently, our data are consistent with a second order transition. Hence, we tried to improve Eq. (7) by replacing the mean-field expression for κ^2 by $\kappa^2 = C_1 \tau^{2\nu}$, where $\tau = (T - T_c)/T_c$ and ν is the exponent for the

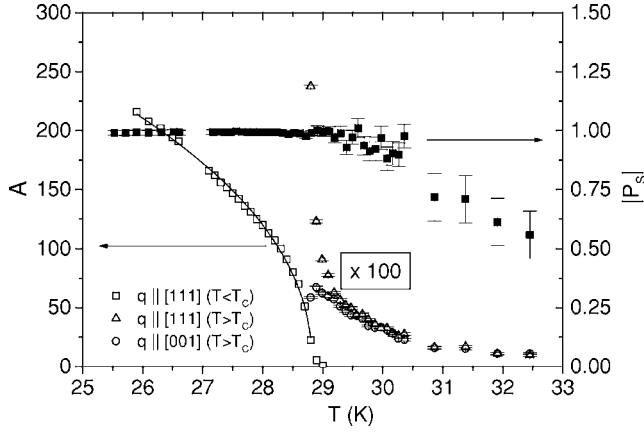


FIG. 3. The temperature dependence of the Bragg intensity and maximal intensities of the critical scattering in the easy ([111]) and hard ([001]) directions (both in different arb. units). The polarization P_s defined by Eq. (8) changes with T at $T > T_c$ and it is constant for Bragg reflections at $T < T_c$.

correlation length for the easy direction. At the same time we introduce the critical exponent for the cubic anisotropy μ by replacing the cubic invariant $\text{Inv} = \{q^4\} - 1/3$ by $(\text{Inv})^\mu$, similar to that in the uniaxial case.¹⁵ Corresponding results are shown in Fig. 5 with $\nu = 0.62(1)$ and $\mu = 0.22(5)$. The fit of the Bragg intensity with $I_B = I_0(-\tau)^{2\beta}$, where β is the critical exponent of the helix magnetization, gives $\beta = 0.22(1)$ (solid line in Fig. 3). The value of β is surprisingly low for the 3D magnetic system but it is close to that found in the frustrated CsMnBr_3 compound, which belongs to the chiral class of universality.^{8,9}

It should be noted that beyond the mean field theory the critical behavior must have two crossovers. At $q \gg k$ one can neglect both the DMI and the AE interactions as in itinerant ferromagnets. Then for $k \sim q$ and $(k-q)^2 > (|F|/B)k^2$ the Brazovskii theory, neglecting AE interaction, should be applicable. Furthermore, for small $(q-k)^2$ and very close to the

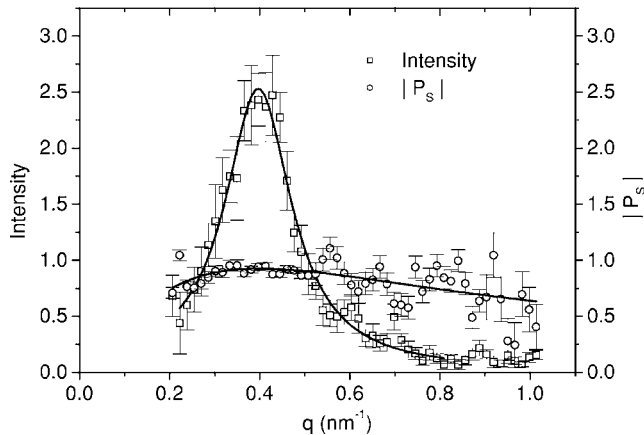


FIG. 4. The q scans across the ring in easy direction for the intensity and P_s at $T_c + 0.3$ K. The solid lines are the best fit results of Eqs. (7) and (8) with $k = 0.39 \text{ nm}^{-1}$ and $\kappa = 0.055 \text{ nm}^{-1}$.

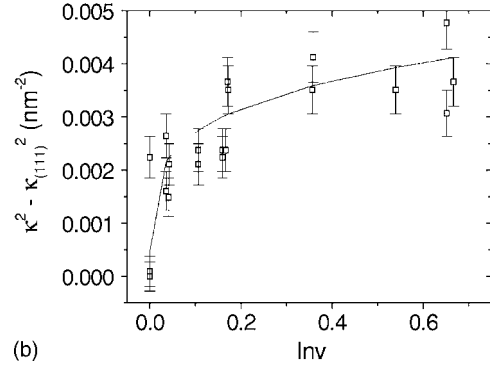
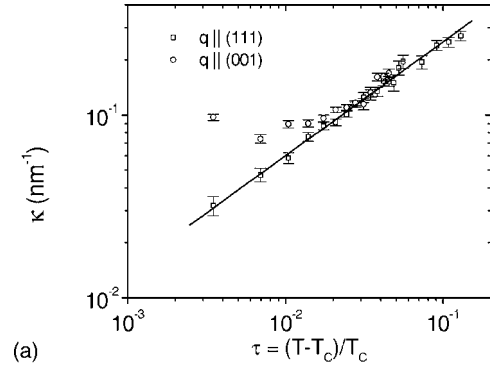


FIG. 5. τ dependence of the inverse correlation length for the easy and hard directions (a). Anisotropic contribution to κ^2 equal to $k^2[(|F|/B)\text{Inv}]^\mu$ as a function of $\text{Inv} = q^4 - 1/3$ (b).

transition one can neglect the $(q-k)^2$ terms in Eqs. (6) and (7) and we will get a behavior determined by the singular properties of $1/\text{Inv}$, which goes to infinity as \mathbf{q} approaches the cubic diagonals. So if $q \rightarrow k$, an additional renormalization group analysis must be done.

We have estimated the parameters B , D and D of the theory. B may be given as $\approx a^2 T_c \approx 50 \text{ meV } \text{\AA}^2$. This estimation is close to the spin-wave stiffness $B \approx 52 \text{ meV } \text{\AA}^2$ measured in the neutron scattering experiment.¹⁷ Further, the helix wave vector $k = D/B = 0.039 \text{ \AA}^{-1}$ for the critical range and therefore $D = 1.9 \text{ meV } \text{\AA}$ and $Da \approx 8 \text{ meV } \text{\AA}^2$. Finally, according to Eq. (6) the inverse correlation length in the hard direction is determined by $\kappa^2 = k^2|F|/(2B)$. From Fig. 5(a) we get $\kappa_{[100]} \approx 0.008 \text{ \AA}^{-1}$ and $|F| = 4 \text{ meV } \text{\AA}^2$. Hence the hierarchy $B > Da > F$ holds at least in rough approximation.

The above results must be compared with the recent investigations of the critical scattering in MnSi at low T and high pressure near the quantum phase transition (QPT). In both cases the maximal scattering intensity lies on a sphere $q = k$, which is the results of the DMI. The Brazovskii theory,¹³ however, is not applicable to the quantum phase transition. The mean-field theory given above is applicable in the high pressure case if one sets $\kappa_0^2 = A(p - p_{c0})$, where A is a constant and p_{c0} is the nonrenormalized critical pressure. The observed transition is of the first order,^{5,6} whereas we observe apparently a second order one. Moreover, near T_c and

p_c the easy axis is directed along [111] and [110], respectively. We believe that these features of the QPT may be connected to the change of the AE interaction under applied pressure.

To conclude, we have a qualitative understanding of the critical fluctuations in MnSi and related compounds FeGe (Ref. 16) and FeCoSi (Ref. 18) but further, more detailed studies, both theoretical and experimental, are demanding.

ACKNOWLEDGMENTS

In conclusion one of the authors (S.M.) is thankful to V. Mineev for interesting discussions. The PNPI and TU-München teams acknowledge GKSS for hospitality. The Russian authors thank RFBR for partial support (Grants Nos. 04-02-16342, 05-02-19889, 03-02-17340, 00-15-96814, and SS-1671.2003.2), “Quantum Macrophysics,” “Collective and Quantum Effects in Condensed Matter,” and Grant “Goscontract 40.012.1.1.1149.”

*Electronic address: grigor@pnpi.spb.ru

†Electronic address: maleyev@sm8283.spb.edu

‡Electronic address: robert.georgii@frm2.tum.de

¹G. Shirane, R. Cowley, C. Majkrzak, J. B. Sokoloff, B. Pagonis, C. H. Perry, and Y. Ishikawa, Phys. Rev. B **28**, 6251 (1983); M. Ishida, Y. Endoh, S. Mitsuda, Y. Ishikawa, and M. Tanaka, J. Phys. Soc. Jpn. **54**, 2975 (1985).

²I. E. Dzyaloshinskii, Zh. Eksp. Teor. Fiz. **46**, 1420 (1964) [Sov. Phys. JETP **19**, 960 (1964)].

³D. Bloch, J. Voiron, V. Jaccarino, and J. H. Wernick, Phys. Lett. **51A** 259 (1975).

⁴T. R. Kirkpatrick and D. Belitz, Phys. Rev. B **67**, 024419 (2003).

⁵C. Pfleiderer, S. R. Julian, and G. G. Lonzarich, Nature (London) **414**, 427 (2001).

⁶C. Pfleiderer, D. Reznik, L. Pintschovius, H. von Lohneysen, M. Garst, and A. Rosch, Nature (London) **427**, 227 (2004).

⁷H. Kawamura, J. Phys.: Condens. Matter **10**, 4707 (1998).

⁸T. E. Mason, B. D. Gaulin, and M. F. Collins, Phys. Rev. B **39**, 586 (1989).

⁹V. P. Plakhty, J. Kulda, D. Visser, E. V. Moskvina, and J. Wosnitza, Phys. Rev. Lett. **85**, 3942 (2000).

¹⁰B. Roessli, P. Boni, W. E. Fisher, and Y. Endoh, Phys. Rev. Lett. **88**, 237204 (2002).

¹¹P. Bak and M. Jensen, J. Phys. C **13**, L881 (1980).

¹²S. V. Maleyev, Physica B **297**, 67 (2001); Phys. Usp. **45**, 569 (2002); Physica B **345**, 119 (2004).

¹³S. A. Brazovskii, Zh. Eksp. Teor. Fiz. **68**, 175 (1975) [Sov. Phys. JETP **41**, 85 (1975)].

¹⁴The real polarization of the scattered neutrons is given by $\sigma(\mathbf{q}, \mathbf{P}_i=0)\mathbf{P}_f = -\partial\sigma/\partial\mathbf{P}_i$ (Ref. 12).

¹⁵E. Riedel and F. Wegner, Z. Phys. **225**, 195 (1969).

¹⁶B. Lebech, in *Recent Advances in Magnetism of Transition Metal Compounds*, edited by A. Kotani and N. Susuki (World Scientific, Singapore, 1993), p. 167.

¹⁷Y. Ishikawa, G. Shirane, J. A. Tarvin, and M. Kohgi, Phys. Rev. B **16**, 4956 (1977).

¹⁸K. Ishimoto, Y. Yamaguchi, J. Suzuki, M. Arai, and M. Furusaka, Physica B **213-214**, 381 (1995).